

Design of an Air-Core Magnet Circuit for a Hall Thruster

William J. Hurley*, Thomas A. Marks† and Benjamin A. Jorns‡
University of Michigan, Ann Arbor MI, 48109

The magnetic field of the SPT-100 is reproduced computationally using an air-core magnetic circuit. The air-core circuit is comprised of a group of solenoids distributed throughout the thruster body. An optimization problem is defined to translate and rotate the solenoids so that the L^2 norm between the measured magnetic field of the SPT-100, and the predicted magnetic field of the solenoids is minimized. The problem is constrained such that the solenoids do not intersect each other or the thruster boundary. It is found that the air-core solution can replicate the design magnetic field with L^2 norm of 11.2 G. The power produced by this circuit was calculated to be 369 W. It was also found that an air-core circuit may reduce the mass of the thruster by >50% compared to traditional ferromagnetic circuits.

I. Nomenclature

A_{sol}	=	Solenoid Area
α	=	Temperature coefficient of resistivity
B_r	=	Radial Magnetic field
B_z	=	Axial Magnetic Field
D	=	Number of Data points
dh	=	Spacing of loops along the height of a solenoid
dw	=	Spacing of loops along the width of a solenoid
E_1	=	Elliptic integral of the first kind
E_2	=	Elliptic integral of the second kind
f	=	Packing Factor
H	=	Height of a Solenoid
I	=	Current of a Current loop
j_{max}	=	Maximum current density in a magnet wire
k	=	Geometric factor
L	=	Swept Length
N	=	Number of Current loops
P	=	Power dissipated
r	=	Radial Location
R	=	Radius of a Current Loop
ρ	=	Resistivity
ρ_0	=	Resistivity at the reference temperature
T	=	Temperature
T_0	=	Reference Temperature
θ	=	Angle of a Solenoid
μ_0	=	permeability of free space
W	=	Width of a Solenoid
z	=	Axial location

II. Introduction

Hall effect thrusters are axisymmetric electric propulsion devices that utilize orthogonal electric and magnetic fields to generate and accelerate a plasma to produce thrust. Moderate power (< 10 kW) Hall thrusters are one of the most

*Ph.D. Candidate, Department of Aerospace Engineering, Student Member AIAA

†Ph.D. Candidate, Department of Aerospace Engineering, Student Member AIAA

‡Associate Professor, Department of Aerospace Engineering, Associate Fellow AIAA

mature and widespread types of in space propulsion flown to date. This stems in large part from their moderately high specific impulses (1500-2000s), high total efficiency (in excess of 60%), long lifetime (>10,000 h), and comparatively high thrust density[1, 2]. These factors have made Hall thrusters attractive candidates to move beyond their current operational envelope and scale to the high powers necessary (>100 kW) for crewed, interplanetary exploration[3].

There are two major technical challenges with increasing the power of thrusters: mass and thrust density scaling. Following commonly accepted design rules [4, 5], a Hall thruster with 2000 s at the 100 kW power level would be over 1 m in diameter with a specific mass ~ 2.5 kg/kW. These figures of merit, while not non-starters for high power applications, can pose major challenges for closing higher power mission architectures [6]. With this in mind, one of the major mass drivers for Hall thrusters is the ferromagnetic material employed to support the magnetic field. If this could be reduced or eliminated, there may be an order of magnitude improvement in specific mass.

Relatedly, another key factor driving the limitation in specific mass is the generally-accepted rule of thumb that Hall thrusters cannot exceed a thrust density greater than 10 N/m^2 [7]. This rule is generally believed to stem from the understanding that higher current density in the thruster channel will lead to unacceptable loss in beam confinement, thereby reducing performance. In principle, this loss could be mitigated by increasing the magnetic field strength in the channel. Indeed, Simmonds and Raitseis [7] predict that for increased applied fields in the channel, the theoretical upper bound of thrust density for these engines could be two orders of magnitude higher than their current limit. The challenge again in achieving this scaling, however, stems from material limitations in the ferromagnets, which often due to saturation effects cannot support magnetic fields in excess of a few hundreds Gauss.

One possible solution to these challenges related to the ferromagnetic circuit is to adopt an air-core configuration. While air-core circuits may require over an order of magnitude more current, they can achieve much higher field strengths while maintaining the desired magnetic field topography. Furthermore, removing the heavy ferromagnetic material in favor of air-cores may reduce the overall specific mass of the thruster. With this in mind, our previous work on an air-core design demonstrated it was possible to replicate a given Hall thruster magnetic field shape and strength with a set of individual current loops[8]. We discretized the Hall thruster body, placing a current loop at each node, and then learned, using Bayesian inference, the set of currents needed to match a given magnetic field.

While this work thus served as a promising initial proof of concept, the results revealed that the practical implementation of the circuit was unfeasible. The required currents in the coils were sufficiently high (>1000 A) as to represent major challenges for energizing and thermally managing them. In light of this previous result, the need was apparent to re-formulate the problem to prioritize finding more physically realizable solutions.

The overall goal of this work is to explore a new approach to achieving this type of field configuration. To this end, we organize this paper in the following way. We first set up a generalized model for our air-core circuit and the framework for matching the field to a target configuration. We then introduce an early, open source version of the SPT-100, which we use as a toy problem to validate our approach. We then present and discuss the results, followed by the main conclusions of this work.

III. Model Definition

Our goal is to use an air-core circuit, one free of ferromagnetic material, to replicate a set of magnetic field data in a Hall thruster channel. To set up this problem, we define a set of solenoids distributed throughout the thruster body. Each solenoid has five parameters that can be adjusted by the optimizer to best match a given magnetic field. These are the r and z location of the center, the height (H) and width (W), and the angle from the horizontal (θ). An example of a solenoid in the 2D channel of a Hall thruster with the parameters labeled is shown in Fig. 1.

We fill each solenoid with equally spaced current loops. The spacing along the width and height of the solenoid, dw and dh , was 0.003 m. This spacing was fine enough so that there was enough loops to properly replicate the field of a solenoid, but not too fine so that the number of generated loops would slow down the optimization. To ensure the solution is feasible, we set the current in each loop to be

$$I_{loop} = j_{max} A_{sol}, \quad (1)$$

where I_{loop} is the current in each loop, j_{max} is the maximum allowable current density in current carrying wire, and $A_{sol} = WH$ is the area of given solenoid. This method for determining the current in each loop ensures that the current does not exceed the limitations of the cabling. Typically, the rule of thumb is that the current should not exceed $\sim 6 \text{ A/mm}^2$ [9]. As an additional benefit, since each solenoid is at the same current density, this results in designs that in principle could be implemented by running all the solenoids from a single power supply.

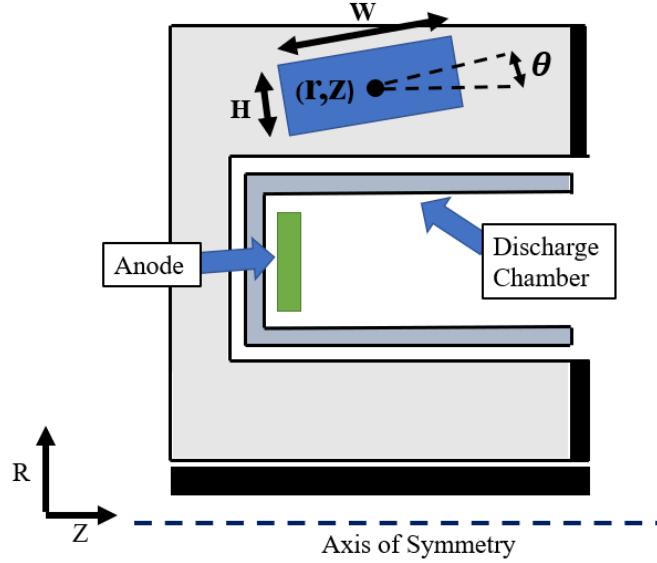


Fig. 1 Example solenoid placed in the Hall thruster body.

To calculate the total magnetic field produced by each solenoid, we use known equations for the magnetic field produced by a loop of current[10]. The axial and radial magnetic field produced by a single loop with current I and radius R centered at $z = 0$ is given by

$$B_z(z, r, I, R) = \frac{\mu_0 I}{2\pi\sqrt{z^2 + (R+r)^2}} \left(\frac{R^2 - z^2 - r^2}{z^2 + (r-R)^2} E_2(k^2) + E_1(k^2) \right) \quad (2)$$

$$B_r(z, r, I, R) = \frac{\mu_0 z I}{2\pi r\sqrt{z^2 + (R+r)^2}} \left(\frac{R^2 - z^2 - r^2}{z^2 + (r-R)^2} E_2(k^2) + E_1(k^2) \right) \quad (3)$$

where μ_0 is the permeability of free space, z and r are the axial and radial distances, respectively, from the loop center, E_1 and E_2 are the elliptic integrals of the first and second kind, and k is a geometric factor defined as

$$k = \sqrt{4rR(z^2 + (R+r)^2)^{-1}} \quad (4)$$

Using these equations for the magnetic field, we can sum over the contributions from each current loop in every solenoid to get a prediction of the magnetic field at a given point in the channel. This can be formally written as

$$\mathbf{B}(z, r) = \sum_{i=1}^N \mathbf{B}(z - Z_i, r, I_i, R_i) \quad (5)$$

where $\mathbf{B} = [B_z(z, r), B_r(z, r)]$ is the magnetic field vector, Z_i is the axial location of current loop i , and N is the total number of current loops. Ultimately, we want to determine the set of solenoids that best match the measured magnetic field. To compute the predicted magnetic field, we sum the magnetic field produced by each current loop in every bobbin at the locations of interest in the channel (locations we have data). To compare how close the predicted magnetic field is to the measurement data, we compute the L^2 norm of the difference between the predicted and measured field, which we define as

$$L^2(\mathbf{x} | d) = \sqrt{\frac{1}{D} \sum_{i=1}^D \|\mathbf{B}_{\text{measured}}(z_i, r_i) - \mathbf{B}(z_i, r_i)\|^2} \quad (6)$$

where D is the number of data points, z_i and r_i are the axial and radial locations, respectively of data point i , $\mathbf{B}_{\text{measured}}$ is the measured magnetic field, and \mathbf{B} is the predicted magnetic field. Therefore, our optimization process will involve

moving around the solenoids so that the L^2 norm is minimized. The solenoids, however, must be constrained to not overlap each other and not leave the thruster body. We can formulate our problem as a constrained optimization problem:

$$\begin{aligned} \min_{\mathbf{x}} L^2(\mathbf{x} | d) \\ \text{s.t. } A_{\text{overlap}}(\mathbf{x}) = 0, \\ A_{\text{out}}(\mathbf{x}) = 0. \end{aligned}$$

Here, \mathbf{x} is the vector of unknowns, i.e. the positions and sizes of the solenoids, A_{overlap} is the sum of the area of overlap between the solenoids, which should be zero in a machinable solution, and A_{out} is the total area of the solenoids outside of the boundary polygon of the thruster, which should be zero if the solenoids lie within the boundary of the thruster. To solve this constrained problem, we can transform it to an unconstrained optimization problem as follows:

$$\min_{\mathbf{x}} L^2(\mathbf{x} | d) + \gamma (A_{\text{overlap}}(\mathbf{x}) + A_{\text{out}}(\mathbf{x})) \quad (7)$$

In the above, \mathbf{x} is the vector of unknowns which we seek to optimize and γ is a *penalty parameter*. By adjusting the penalty parameter, we can control the importance of minimizing the objective versus adhering to the constraints. Our optimization thus proceeded as follows:

- 1) Solve optimization problem with low γ
- 2) Increase γ
- 3) Use solution with lower γ to solve with higher γ
- 4) Repeat until the constraints are satisfied and the solution is satisfactory

To solve the local optimization problem, we employed the Optim[11] package for the Julia programming language. We used the LBFGS algorithm with a second-order backtracking linesearch. The main tuning parameter in the solution is the value of γ . We started with an initial γ of 10,000 and then increased it subsequently to 500,000 properly penalize solutions which the bobbins intersected each other or were outside of the channel.

IV. SPT-100 as an Example Case

Now that we have established the relevant background and framework for our analysis, we consider a case study to demonstrate its capabilities. We attempt to match the magnetic field of the SPT-100 with an air-core circuit. The SPT-100 is a low power <1.5 kW Hall thruster developed originally by FAKEL [12]. It has been operated extensively since the 90's in both laboratory settings and in space. This thruster has an open source design, and a picture of the SPT-100 with a labeled, projected 2-D cross section is shown in Fig. 2.

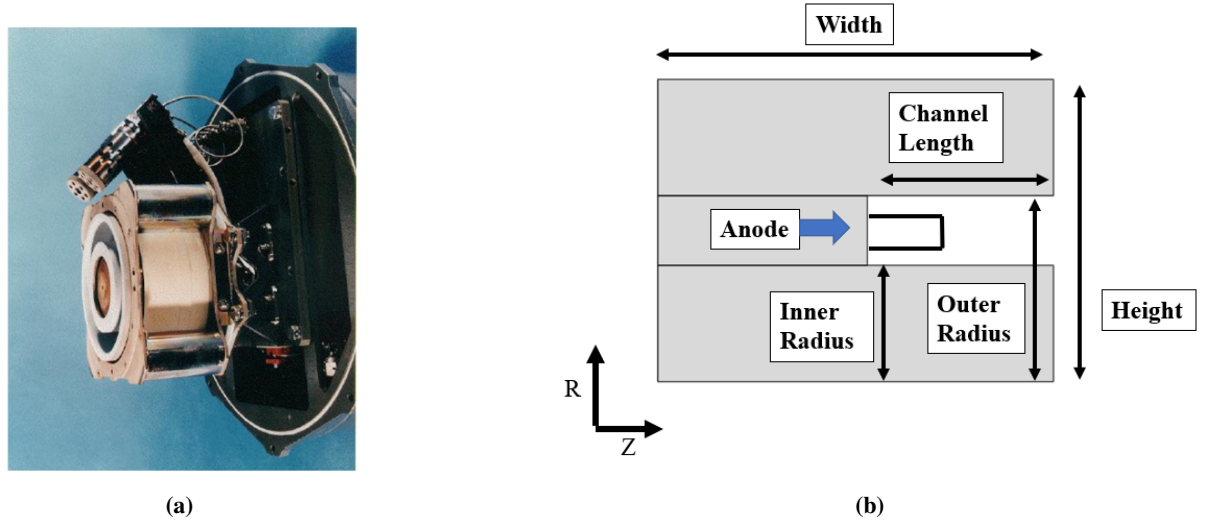


Fig. 2 The SPT-100 Hall thruster and an example 2-D cross section.

To account for the discharge chamber, we use a larger value for the outer radius and smaller value for the inner radius. This will ensure that the penalty terms in the optimizer accurately penalize solutions where the bobbins would intersect the discharge chamber or channel. The magnetic field data for the SPT-100 was extracted from the results of the Finite Element Method Magnetics (FEMM) model available through the HALLIS project [13].

V. Results

In this section, we attempt to match the magnetic field of the SPT-100, using a set of solenoids, all fixed to the same current density. To start, we initialize the solution by forming a set of solenoids distributed throughout the body of the SPT-100. Each solenoid is composed of a set of equally spaced current loops, all at the same current. The initial condition is plotted in Fig. 3.

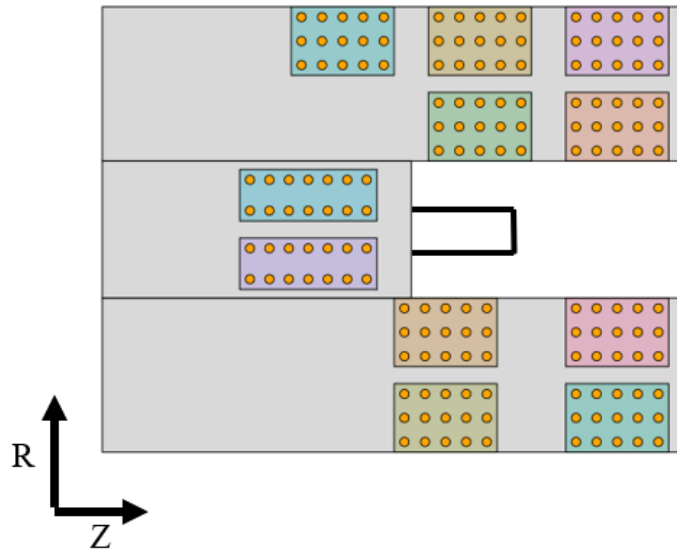


Fig. 3 Initial solenoid placement throughout the body of the SPT-100. The individual current loops are represented as orange circles within each solenoid.

The optimizer then moves around these initially placed solenoids to find the set that best matches a given field. The resulting magnetic field lines in the channel and radial field along centerline of the SPT-100 are compared to that predicted by the air-core circuit in Fig. 4. The axis of Fig. 4a have been normalized to the radius of the outer channel and the axial location of the exit plane. Similarly, the axis of Fig. 4b have been normalized to the peak measured radial magnetic field and the axial location of the exit plane.

The resulting L^2 norm between the measurement data and predicted field for this solution was 11.2 G. Looking at the field lines, we see that the air-core circuit replicates the SPT-100 magnetic field near the exit plane. The worst agreement is near the anode and near the outer channel radius. Since the strength of the magnetic field is relatively low in this region, small differences in B_z or B_r can cause the streamline shape to change significantly more than those same differences would cause in a high magnetic field region.

The peak radial center-line field must be sufficiently strong so that electrons remain locally confined to the acceleration region. The radial magnetic field along centerline generated by the air-core circuit matches the measurement data in the middle of the channel to within 1%, but begins to differ near the exit plane and anode. Near the anode, we see that the air-core circuit produced a stronger radial magnetic field than measured, and at the exit plane it produced a weaker field. Indeed, the air-core circuit magnetic field is smaller than the measured SPT-100 data by 9.1 % at the exit plane. Since the magnetic field is linearly proportional to the current used in each loop, simply scaling the currents could make up for this difference in the peak field. The distribution of solenoids that generated this field is shown in Fig. 5.

Comparing with the initial placement, we see that the area for the set of solenoids placed above the channel was reduced. The two solenoids placed behind the channel moved slightly downward, with one of them having one more row of current loops. The set of solenoids below the channel remained close to each other, and in some cases slightly overlapped. Furthermore, one of the solenoids extends partially into the discharge chamber, which could be an issue if

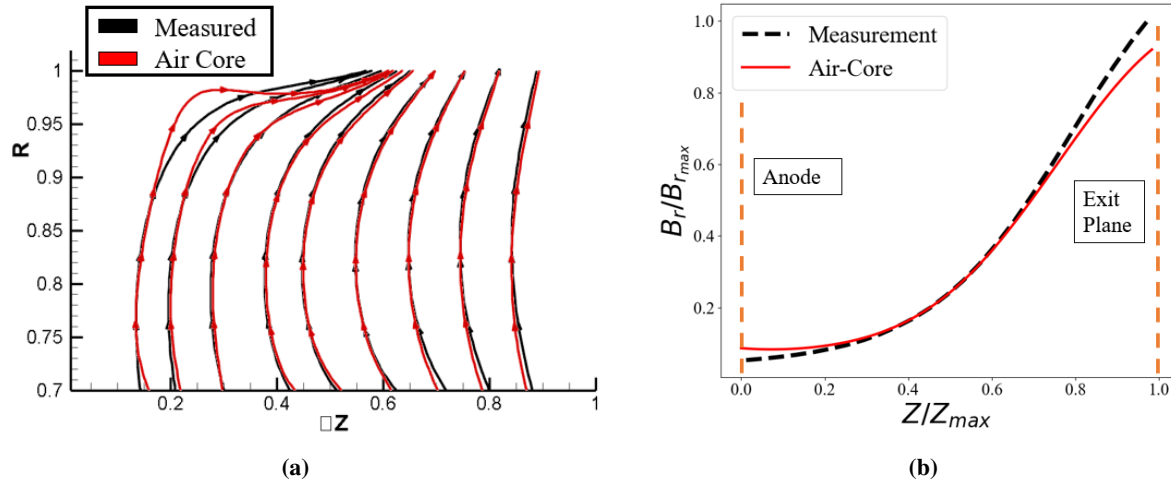


Fig. 4 The SPT-100 (black) a) magnetic field in the channel and b) radial field strength along centerline is compared to an air-core circuit (red).

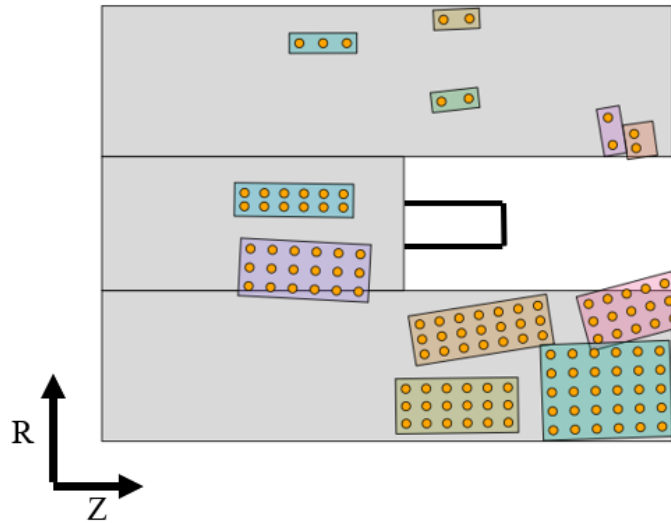


Fig. 5 Final solenoid placement of the air-core circuit used to replicate the SPT-100 magnetic field.

we attempted to build this configuration. Since the magnetic field produced by a current loop decreases with distance, the optimal solenoid placement for an accurate solution is as close to the region of high magnetic field as possible. Indeed, using smaller values for the penalty factor (γ), resulted in more accurate solutions, but the solenoids significantly overlapped one another and protruded into the discharge chamber toward regions of high magnetic field.

VI. Discussion

In the previous section, we showed that a set of solenoids fixed to the same maximum current density can match the magnetic field reasonably well. Fixing the current density makes building this circuit more feasible as all the solenoids may be able to be run off the same power supply. Similarly, this formulation also ensures we do not exceed the limits of the cabling. In this section we look in more detail at the final solution. This includes the power dissipated, a discussion on the maximum current density in magnet wires, and the potential thruster weight savings with an air-core circuit.

A. Power Dissipated

The power dissipated in the magnetic circuit impacts the overall thruster efficiency and thermal loading. Any power spent not accelerating ions is an efficiency loss. An air-core circuit will inherently dissipate more power in the electromagnetic circuit than traditional Hall thrusters, which use ferromagnetic material to amplify the field. To estimate the power dissipated in the air-core circuit, we model the power consumed by each solenoid. This is formulated as

$$P = I^2 \frac{\rho L}{A_{sol} f}. \quad (8)$$

where I is the current for each loop in the solenoid, L is the swept length of the solenoid, f is the packing factor for the magnet wire, and ρ is the resistivity of the conductor material. The current is set by multiplying the maximum current density (6 A/mm^2) by the solenoid area $A_{sol} = WH$. The swept length of each solenoid is $2\pi r$, where r is the solenoid center. The packing factor f accounts for the fact that the total area of each bobbin will not be completely filled with the conductor material. We assume a packing factor of 0.9 for this analysis. We also assume that the conductor material used in each loop is copper, and that its resistivity is a linear function of the operating temperature. The resistivity can then be defined as

$$\rho = \rho_0(1 + \alpha(T - T_0)), \quad (9)$$

where ρ_0 is the resistivity at the reference temperature T_0 , and α is the temperature coefficient of resistivity. For copper, ρ_0 at 20 C is $1.724 * 10^{-8} \Omega\text{-m}$, and $\alpha = 4.29 * 10^{-3} \text{ 1/C}$ [14]. We also assume that the operating temperature of the magnetic circuit is $\approx 500 \text{ C}$. While we do not know the actual temperature that these coils will be at, typical high temperature magnet wire insulation is rated to about 500 C. Summing over the power dissipated by each solenoid at this temperature, we find a total dissipated power of **369 W**.

Since the resistance of the wire increases with temperature, we can potentially reduce the total power used by efficiently rejecting the heat produced by the magnets. Similarly, a large amount of heat will be produced by the plasma, especially at high current densities. Therefore, keeping the magnet wire thermally isolated from the plasma is imperative to operation. Looking at the final placement of the solenoids (Fig. 5), we see that one of them intersects the discharge chamber. This could be a potential issue to build and keep thermally isolated from the channel.

Overall, the power dissipated by the air-core circuit is going to be higher than its ferromagnetic counterpart, but this power likely will be able to be rejected passively. However, since the power scales quadratically with current, higher magnetic field strengths may cause a significant increase in the power dissipated. Indeed, if we increase the magnetic field strength by a factor of 3 by scaling the currents, the total power dissipated is **3329 W**. This is a dominant loss process for small thrusters like the SPT-100 (discharge power of 1.35 kW) but may be acceptable for higher power systems.

B. Maximum Current Density

We formulated this optimization problem so that each solenoid was fixed to the same maximum current density of 6 A/mm^2 . This upper bound is not the same for every application, and is directly coupled to the configuration that the wires are in. The main limiting factor on current density is the insulation of the wires. If the insulation fails due to high thermal loads, the conductor material could be exposed. This could lead to a loss of total turns in the solenoid and a resulting change in the magnetic field produced. Therefore, keeping the temperature of the magnet wire below its rated value is imperative to a robust air-core magnetic field design.

The maximum possible current density in the magnet wire will depend heavily on our configuration of solenoids, and any cooling schemes we have in place. Once a final solenoid configuration is determined, the circuit, plasma loading, and cooling schemes should be thermally modeled in a software like COMSOL to get a high fidelity prediction of the loading. This will give a better estimate on what the maximum current density can be and therefore how much the magnetic field strength can be increased.

C. Thruster Mass

Decreasing the specific mass of the thruster will be key to enable more rapid acceleration, necessary for crewed travel. One added benefit of an air-core circuit is the removal of the heavy ferromagnetic material, leading to a potential decrease in specific mass. In this section we attempt to quantify the potential mass savings with using an air-core design, versus one with ferromagnetic material.

To calculate the mass of our air-core circuit, we use the swept volume generated by each solenoid, multiplied by the density of copper which is 8830 kg/m^3 . This results in a total mass of 1.55 kg. If we assume the support structure for the solenoids is $\sim 25\%$ of the solenoid mass, then the structure plus the solenoids is $\sim 2 \text{ kg}$.

The total mass of the SPT-100 is 5.6 kg [15], with the majority of this weight made up by the ferromagnetic material and magnet wire. If we assume that 90% of the SPT-100 mass is the ferromagnetic material and solenoids, then 0.56 kg is reserved for the other components. Therefore this thruster with an air-core circuit would have a total mass of $\sim 2.5 \text{ kg}$, which is 55% less than with ferromagnetic material. This decrease in specific mass could make Hall thrusters with air-core magnetic circuits ideal options for mission pulls that require increased acceleration.

While in principal an air-core circuit by itself may reduce the thruster mass, we did not account for any passive cooling components that may be needed to reject the increased heat produced. Indeed, as we push the limits on the maximum current density in the magnet wire, these cooling schemes may become more pertinent.

VII. Conclusion

We demonstrated that an air-core circuit comprised of a set of solenoids can replicate the magnetic field of a Hall thruster. The magnetic field of air-core circuits are not limited by saturation in the ferromagnetic material, in principal allowing for higher field strengths. To design this circuit, we used a set of solenoids, all fixed to the same maximum current density of a magnet wire. Fixing the current density may allow for all the solenoids to be run off of a single power supply, rather than having an individual supply for each. Each solenoid was comprised of infinitesimally small, equally spaced current loops. Using the known equations for the magnetic field of a current loop, we calculated the magnetic field produced by each solenoid. The SPT-100 Hall thruster geometry and magnetic field were used to test the validity of this approach. The optimizer moved around and changed the size of each solenoid until the magnetic field produced best matched the measured data. A penalty term was used to penalized solutions in which the solenoids intersected each other or the boundary of the thruster. The results demonstrated that the shape of the magnetic field lines can be closely matched, but that the peak radial field in the channel was 9.1 % smaller for the air-core circuit. The final placement of the solenoids revealed that one solenoid intersected the inner part of the discharge chamber, which may make it difficult to machine in the current configuration. The power produced by this circuit was 369 W, which likely will be able to be passively rejected. Since the power scales quadratically with the current used, increasing the magnetic field by 3 times results in a power dissipation of 3329 W. This is prohibitively high for state of the art Hall thrusters at moderate power but may be acceptable at higher power densities. We also showed that an air-core circuit might offer substantial mass savings ($>50\%$) compared with circuits that use ferromagnetic material. For future iterations on this design, it is likely that varying the total amount of solenoids in the initialization in conjunction with more careful tuning of the penalty parameter (γ), could lead to a even higher fidelity magnetic field, with the solenoids not intersecting the thruster boundary.

References

- [1] Goebel, D., and Katz, I., *Fundamentals of Electric Propulsion: Ion and Hall Thrusters*, John Wiley and Sons, 2008.
- [2] Mikellides, I., Katz, I., Hofer, R., and Goebel, D., “Magnetic Shielding of a Laboratory Hall thruster,” *Journal of Applied Physics*, Vol. 115, No. 043303, 2014. <https://doi.org/10.1063/1.4862313>.
- [3] “Space Nuclear Propulsion for Human Mars Exploration,” *National Academies of Sciences*, 2021.
- [4] Dannenmayer, K., and Mazouffre, S., “Elementary Scaling Relations for Hall Effect Thrusters,” *Journal of Propulsion and Power*, Vol. 27, No. 1, 2011, pp. 236–245. <https://doi.org/10.1051/eucass/201102601>.
- [5] Hofer, R., and Randolph, T., “Mass and cost model for selecting thruster size in electric propulsion systems,” *Journal of Propulsion and Power*, Vol. 29, No. 1, 2013, pp. 166–177.
- [6] Dankanich, J., Vondra, B., and Ilin, A. V., “Fast transits to Mars using electric propulsion,” *46th AIAA/ASME/SAE/ASEE Joint Propulsion Conference and Exhibit*, 2010.
- [7] Simmonds, J., Raitses, Y., and Smolyakov, A., “A Theoretical Thrust Density Limit for Hall Thrusters,” *Physics of Plasmas*, 2022.
- [8] Hurley, W., Marks, T., Gorodetsky, A., and Jorns, B., “Application of Bayesian Inference to Design and Air-Core Circuit for a Magnetically Shielded Hall Thruster,” *International Electric Propulsion Conference*, 2022.
- [9] “Current Carrying Capacity of Copper Conductors,” <https://www.multicable.com/resources/reference-data/current-carrying-capacity-of-copper-conductors/>, 2017.
- [10] Simpson, J., Lane, J., Immer, C., and Youngquist, R., “Simple Analytic Expressions for the Magnetic Field of a Circular Current Loop,” 2013.
- [11] Mogensen, P. K., and Riseth, A. N., “Optim: A mathematical optimization package for Julia,” *Journal of Open Source Software*, Vol. 3, No. 24, 2018, p. 615. <https://doi.org/10.21105/joss.00615>, URL <https://doi.org/10.21105/joss.00615>.
- [12] Sankovic, J., Hamley, J., and Haag, T., “Performance Evaluation of the Russian SPT-100 Thruster at NASA LeRC,” *23rd International Electric Propulsion Conference*, 1993.
- [13] “Hall Ion Sources Simulation Software,” <https://www.hallis-model.com/>, 2022.
- [14] “Resistivity and Conductivity-Temperature Coefficients of Common Materials,” https://www.engineeringtoolbox.com/resistivity-conductivity-d_418.html, 2003.
- [15] Gnizdor, R., komarov, A., Mitrofanova, O., Saevets, P., and Semenenko, D., “High Impulse SPT-100D Thruster with Discharge Power of 1.0...3.0 kW,” *35th International Electric Propulsion Conference*, 2017.